Atmosphere-Ocean
Publication details, including instructions for authors and subscription information:
http://www.tandfonline.com/loi/tato20

Measurements of CO, HCN, and C_2H_6 Total Columns in Smoke Plumes Transported from the 2010 Russian Boreal Forest Fires to the Canadian High Arctic

C. Viatte[a], K. Strong[a], C. Paton-Walsh[b], J. Mendonca[a], N. T. O'Neill[c] & J. R. Drummond[ad]

[a] Department of Physics, University of Toronto, Toronto, Ontario, Canada

[b] Department of Chemistry, University of Wollongong, Wollongong, New South Wales, Australia

[c] Centre for Research and Applications in Remote Sensing, Université de Sherbrooke, Sherbrooke, Quebec, Canada

[d] Department of Physics and Atmospheric Sciences, Dalhousie University, Halifax, Nova Scotia, Canada

Published online: 02 Aug 2013.

To cite this article: C. Viatte, K. Strong, C. Paton-Walsh, J. Mendonca, N. T. O'Neill & J. R. Drummond (2013) Measurements of CO, HCN, and C_2H_6 Total Columns in Smoke Plumes Transported from the 2010 Russian Boreal Forest Fires to the Canadian High Arctic, Atmosphere-Ocean, 51:5, 522-531, DOI: 10.1080/07055900.2013.823373

To link to this article: http://dx.doi.org/10.1080/07055900.2013.823373

Measurements of CO, HCN, and C_2H_6 Total Columns in Smoke Plumes Transported from the 2010 Russian Boreal Forest Fires to the Canadian High Arctic

C. Viatte[1,*], K. Strong[1], C. Paton-Walsh[2], J. Mendonca[1], N. T. O'Neill[3] and J. R. Drummond[1,4]

[1]*Department of Physics, University of Toronto, Toronto, Ontario, Canada*
[2]*Department of Chemistry, University of Wollongong, Wollongong, New South Wales, Australia*
[3]*Centre for Research and Applications in Remote Sensing, Université de Sherbrooke, Sherbrooke, Quebec, Canada*
[4]*Department of Physics and Atmospheric Sciences, Dalhousie University, Halifax, Nova Scotia, Canada*

[Original manuscript received 25 January 2013; accepted 4 June 2013]

ABSTRACT *In August 2010, simultaneous enhancements of aerosol optical depth and total columns of carbon monoxide (CO), hydrogen cyanide (HCN), and ethane (C_2H_6) were observed at the Polar Environment Atmospheric Research Laboratory (PEARL, 80.05°N, −86.42°W, 0.61 km above sea level, Eureka, Nunavut, Canada). Moderate Resolution Imaging Spectroradiometer (MODIS) hot spots, Ozone Monitoring Instrument (OMI) aerosol index maps, and Hybrid Single Particle Lagrangian Integrated Trajectory (HYSPLIT) back-trajectories were used to attribute these enhancements to an intense boreal fire event occurring in Russia. A ground-based Fourier Transform InfraRed (FTIR) spectrometer at PEARL provided vertically integrated measurements of trace gases transported in smoke plumes. We derived HCN and C_2H_6 equivalent emission ratios with respect to CO of 0.0054 ± 0.0022 and 0.0108 ± 0.0036, respectively, and converted them into equivalent emission factors of 0.66 ± 0.27 g kg^{-1} and 1.47 ± 0.50 g kg^{-1} (in grams of gas per kilogram of dry biomass burnt, with one-sigma uncertainties). These emission factors add new observations to the relatively sparse datasets available and can be used to improve the simulation of biomass burning fire emissions in chemical transport models. These emission factors for the boreal forest are in agreement with the mean values recently reported in a compilation study.*

RÉSUMÉ *[Traduit par la rédaction] En août 2010, des enrichissements simultanés de l'épaisseur optique des aérosols et de l'épaisseur totales des colonnes de monoxyde de carbone (CO), de cyanure d'hydrogène (HCN) et d'éthane (C_2H_6) ont été observés au Laboratoire de recherche atmosphérique en environnement polaire (PEARL, 80,05°N, −86,42°O, 0,61 km au-dessus du niveau de la mer, Eureka, Nunavut, Canada). Nous avons utilisé des points chauds de spectroradiomètre imageur à résolution moyenne (MODIS), des cartes d'indices d'aérosols d'un instrument de surveillance de l'ozone (OMS) et les rétrotrajectoires fournies par le HYSPLIT (Hybrid Single Particle Lagrangian Integrated Trajectory) pour attribuer ces enrichissements à un feu de forêt boréale intense se produisant en Russie. Un spectromètre infrarouge à transformée de Fourier (FTIR) au sol au PEARL a fourni des mesures verticalement intégrées de gaz traces transportés dans les panaches de fumée. Nous avons dérivé des rapports d'émission équivalents de HCN et de C_2H_6 par rapport au CO de 0,0054 ± 0,0022 et 0,0108 ± 0,0036, respectivement, et les avons convertis en facteurs d'émission équivalents de 0,66 ± 0,27 g kg^{-1} et 1,47 ± 0,50 g kg^{-1} (en grammes de gaz par kilogramme de biomasse sèche brulée, avec des incertitudes de 1 sigma). Ces facteurs d'émission ajoutent de nouvelles observations aux assez rares ensembles de données disponibles et peuvent servir à améliorer les simulations d'émissions lors de feux de biomasse dans les modèles de transport chimique. Ces facteurs d'émission pour la forêt boréale s'accordent avec les valeurs moyennes récemment publiées dans une étude de compilation.*

KEYWORDS atmosphere; FTIR measurements; Arctic; biomass burning; boreal fire; emission factors; PEARL; CANDAC

[*]Corresponding author's email: viatte@atmosp.physics.utoronto.ca

1 Introduction

Fires release considerable amounts of radiatively and photochemically active trace gases, such as carbon monoxide (CO), hydrogen cyanide (HCN), and ethane (C_2H_6), as well as aerosols (IPCC, 2007; Zhao et al., 2002). It has been suggested that biomass burning is an important source of Arctic pollution; boreal fires in Siberia, Canada, and Alaska represent a major perturbation to the Arctic atmosphere in summer, affecting the carbon cycle (Preston & Schmidt, 2006), climate (Amiro et al., 2001), air quality (Colarco et al., 2004), and land ecology (Soja et al., 2007). Several studies have identified pollution transport of biomass burning products to the Arctic on the basis of model simulations (e.g., Shindell et al., 2008) and aerosol observations (e.g., Saha et al., 2010), but our ability to observe fire plumes in terms of vertically integrated chemical composition has been limited. The Polar Environment Atmospheric Research Laboratory (PEARL) located at Eureka, Nunavut, Canada, is appropriately situated for sampling the outflow of boreal biomass burning pollution over the Arctic region and is equipped with a Fourier Transform InfraRed (FTIR) spectrometer and a sunphotometer to measure trace gases and aerosols, respectively. To quantify the atmospheric impact of biomass burning in chemical transport models, emission factors of trace gases must be implemented accurately, but those factors are highly variable because they depend on the types of vegetation burned, the combustion phase (smouldering and flaming), and on atmospheric conditions at the time of the fire events (Paton-Walsh et al., 2004, 2005, 2010; Vigouroux et al., 2012). Given their long lifetimes, HCN and C_2H_6 are considered to be tracers of pollution transport such as that associated with biomass burning plumes. Within the past decade, measurements of emission factors of HCN and C_2H_6 have led to a wide range of values, which may be a result of the natural variability of the emissions and/or the discrepancies between sampling methods (laboratory, airborne, satellite, and ground-based measurements) that overestimate or underestimate the combustion phases (smouldering and flaming). Andreae and Merlet (2001) stressed the need for more measurements of HCN emission factors given the value of HCN as a biomass burning tracer (Li et al., 2003). Concerning C_2H_6, recent work shows that biomass fires emit more non-methane hydrocarbons (including C_2H_6) than previously thought and that this may improve the chemical model performance (Akagi et al., 2011).

That is why, in this study, precise FTIR measurements of trace gas columns inside smoke plumes were used to assess emission factors in order to add new observations to the sparse datasets that have been reported and compiled in the literature (Akagi et al., 2011; Andreae & Merlet, 2001).

2 Measurements and analysis

a *FTIR Measurements*

The FTIR spectrometer (Bruker IFS 125HR) located at PEARL has been operational since August 2006 and is part of the Network for the Detection of Atmospheric Composition Change (NDACC; http://www.ndsc.ncep.noaa.gov/) and the Total Carbon Column Observing Network (TCCON; http://www.tccon.caltech.edu/). Trace gas columns such as biomass burning products CO, HCN, and C_2H_6 have been derived from individual solar absorption spectra in the middle infrared region for NDACC (2057.7–2159.3 cm^{-1} for CO, 3268.0–3287.5 cm^{-1} for HCN, and 2976.6–2987.0 cm^{-1} for C_2H_6) and in the near infrared region for TCCON (4233–4290 cm^{-1} for CO) (Batchelor et al., 2009; Lindenmaier, 2012). The NDACC and TCCON measurements were made successively because beamsplitters had to be changed for acquisition. The High Resolution TRANsmission HITRAN 2008 line parameters (Rothman et al., 2009) were used in both the NDACC and TCCON analyses and all the interfering species inside these micro-windows were scaled from a priori profiles.

For the NDACC measurements, total columns of all three molecules were retrieved using the iterative fitting algorithm SFIT2 (Rinsland et al., 1998) based on the Optimal Estimation Method (OEM) of Rodgers (2000), with a priori Volume Mixing Ratio (VMR) profiles for every gas based on the mean of a 40-year run (1980–2020) from the Whole Atmosphere Chemistry Climate Model (WACCM, version 5, Eyring et al. (2007)) for Eureka (J. Hannigan, National Center for Atmospheric Research, personal communication, 2012). The retrieved vertical profiles were obtained on a 48-level altitude grid (from 0.61 to 120 km). Total columns were then derived by vertically integrating retrieved profiles. The diagonal elements of the a priori covariance matrix were used as a tuning parameter (i.e., they were optimized empirically to stabilize the retrievals and maximize the spectral information). We used 50%, 20%, and 30% as the one-sigma variability to generate the diagonal elements of the covariance matrices for HCN, CO, and C_2H_6, respectively. These values are consistent with the natural tropospheric variabilities derived from the WACCM model.

Full error analysis is performed following the formulation of Rodgers (2000). The analysis can be divided into three different error sources: the smoothing error expressing the uncertainty caused by the limited vertical resolution of the retrieval, the forward model parameter error, and the measurement noise error. Typical total uncertainties on total columns (including smoothing, temperature, and measurement errors, spectroscopic line width and line intensity uncertainties, and solar zenith angle error, added in quadrature) are 2.5%, 9.0%, and 3.5% for CO, HCN, and C_2H_6, respectively. The average degrees of freedom for signal, over the 2007 to 2011 period, are 2.8, 1.6, and 1.9 for CO, HCN, and C_2H_6 total columns, respectively. For the TCCON retrievals of CO, the non-linear least-squares fitting algorithm GFIT is used to scale a priori VMR profiles, which are derived from Atmospheric Chemistry Experiment-Fourier Transform Spectrometer (ACE-FTS) climatology, in order to generate the best spectral fit, with a total column error of 2% (Wunch et al., 2011). During the fire event of August 2010, 61 individual

middle infrared spectra were recorded through the smoke plume from 9 to 30 August 2010; the 41 near-infrared spectra recorded on 23 August confirmed the rapid enhancement of CO columns on that day. Smoke aerosol is not explicitly included in the spectral fits given that any spectral signatures will be broad compared with the narrow fitting micro-windows. To optimize the quality of the retrievals, both NDACC and TCCON spectra and fits have to satisfy quality filters based on signal-to-noise ratios, baseline distortions, and fitting residuals.

b *Aerosol Measurements*

Spectral solar irradiance and almucantar radiance is measured by a Cimel sunphotometer/sky radiometer belonging to the Aerosol Canada network and the Aerosol Robotic Network (AEROCAN/AERONET; AEROCAN is a federated Canadian subnetwork of the worldwide AERONET network led by the National Aeronautics and Space Administration (NASA, http://aeronet.gsfc.nasa.gov). It is located at PEARL and has been operational since March 2007. The Cimel instrument, as well as AERONET measurement protocols, are described by Holben et al. (1998). The PEARL Aerosol Optical Depths (AODs) are acquired in a high-frequency (3-minute) temporal mode. Total, fine, and coarse mode AODs at 500 nm are retrieved using the Spectral Deconvolution Algorithm (SDA, AERONET Version 2.0) of O'Neill, Eck, Smirnov, Holben, and Thulasiraman (2003). We used level 2.0 AERONET to ensure data quality control.

c *Infrared Atmospheric Sounding Interferometer (IASI) Satellite Measurements*

Global CO concentrations are retrieved daily from spaceborne Infrared Atmospheric Sounding Interferometer (IASI) radiance spectra using the Fast Optimal Retrievals on Layers for IASI (FORLI) software (Hurtmans et al., 2012; Turquety et al., 2009). The quality of FORLI-CO retrievals has been evaluated for highly polluted conditions caused by wildfires (Turquety et al., 2009) and more recently by comparison with NDACC FTIR measurements (Kerzenmacher et al., 2012). Data are available at http://ether.ipsl.jussieu.fr/php/test2.php.

d *Calculation of Emission Factors*

Trace gas concentrations within smoke plumes vary rapidly with time, so a common way of deriving an emission factor is to measure the emission ratio of the target chemical species relative to a reference species, which is often carbon dioxide (CO_2) or CO (Hurst, Griffith, & Cook, 1994). In our study we used CO as the reference because variations in CO_2 concentration are difficult to measure with sufficient accuracy. Because the emission ratio was not measured at the source of the fire, it is more accurately called an "enhancement ratio." These ratios are derived from the regression slope of a given trace gas total column versus that of CO.

For comparison with previous studies, our enhancement ratios (i.e., equivalent emission ratios) were converted into equivalent emission factors using (Andreae & Merlet, 2001):

$$\mathrm{EF}_x = \mathrm{ER}_{(x/\mathrm{CO})} \times \left(\frac{\mathrm{MW}_x}{\mathrm{MW}_{\mathrm{CO}}}\right) \times \mathrm{EF}_{\mathrm{CO}}, \qquad (1)$$

where EF_x is the emission factor for trace gas x in grams of gas per kilogram of dry biomass burnt; $ER_{(x/CO)}$ is the molar emission ratio of trace gas x with respect to CO; MW_x is the molecular weight of trace gas x; MW_{CO} is the molecular weight of CO, and EF_{CO} is the emission factor of CO.

In this study, values of EF_{CO} of 127 ± 45 g kg^{-1} and 107 ± 37 g kg^{-1} for dry matter based on Akagi et al. (2011) and Andreae and Merlet (2001), respectively, were taken as the mean emission factor for CO for boreal and extratropical forests because this is the fuel type of the source fires. Uncertainties in the measured EF_{CO} were calculated by taking into account the large uncertainty in the CO emission factor (more than 35%) and the uncertainty in the calculated regression slope (7.9% and 5.0% for HCN and C_2H_6, respectively), as well as the total uncertainties of the retrievals, all combined in quadrature (Paton-Walsh et al., 2005).

3 Measurement of biomass burning products

a *Trace Gas Total Columns and AODs at Eureka in August 2010*

Figure 1a presents the time series of the FTIR total columns of CO (both TCCON and NDACC), HCN, and C_2H_6 from 9 to 30 August 2010, where simultaneous enhancement of the three biomass burning species, with a sharp increase on 23 August (yellow box) and persistent elevated concentrations from that day to 29 August, can be seen. Focusing on 23 August, Fig. 1b shows that the CO total columns measured by the FTIR increase from 1.8×10^{18} molecules cm^{-2} at 1500 UTC to 2.1×10^{18} molecules cm^{-2} at 2200 UTC on that day. Furthermore, Fig. 1c shows the distribution of the IASI CO total column over the Eureka area on 23 August, where a local enhancement of CO is clearly observed. The higher IASI CO total columns could be caused by the potential bias of the thermal emission instrument sensitivity, which is higher in summer (Eremenko et al., 2008). In addition, Fig. 1b shows that fine-mode AODs increase throughout that day whereas coarse-mode AODs remain constant. This suggests the presence of a smoke plume inasmuch as fine-mode AODs can be traced to fire events, whereas coarse-mode AODs are characteristic of thin homogeneous clouds, marine aerosols, ash, and/or dust in the atmosphere. This event is significant but rather weak in terms of smoke-induced, fine-mode AOD variation at Eureka; the variation, less than 0.04, is comparable to the late-spring or summer observations made by O'Neill et al. (2008) but significantly less than the strong springtime smoke events observed by Saha et al. (2010) during the Arctic Research of the Composition of the

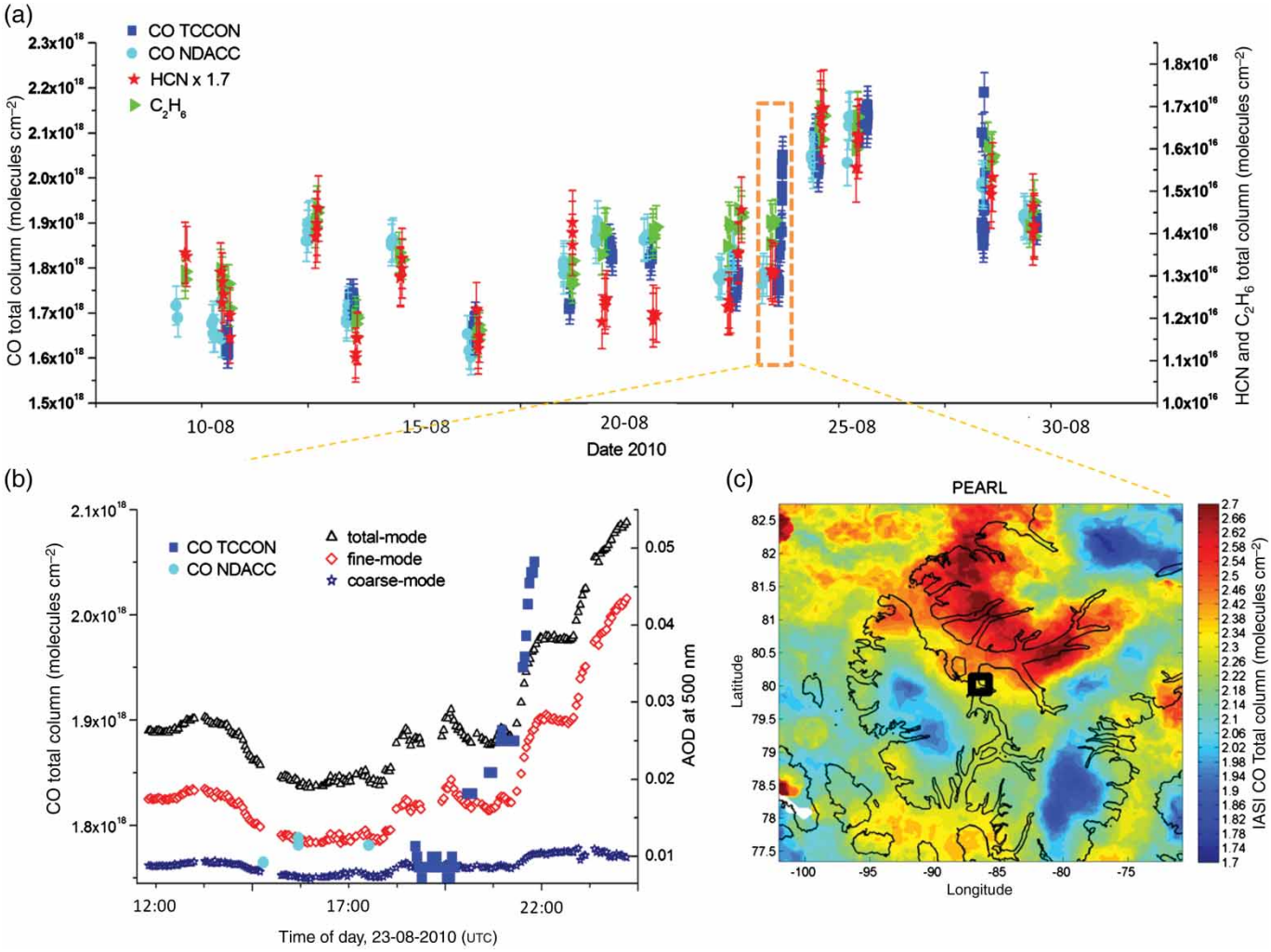

Fig. 1 Trace gas total columns and AODs measured at PEARL in August 2010. (a) Time series of FTIR total columns of CO (from TCCON in blue and NDACC in cyan), HCN (in red, scaled by a factor of 1.7) and C_2H_6 (in green) from 9 to 30 August 2010. Error bars indicate the total column uncertainties of 2.5% (and 2%), 9.0%, and 3.5% for CO (and TCCON CO), HCN, and C_2H_6, respectively. The 23 August 2010 is outlined by the dark yellow box. (b) Time series of CO total columns (FTIR measurements in blue: TCCON in blue and NDACC in cyan) and total, fine- and coarse-mode AODs at 500 nm derived from AERONET (in black, red, and dark blue, respectively) plotted for 23 August 2010. (c) Distribution of CO total columns measured by IASI within 550 km of Eureka (indicated by the black box) for the same day.

Troposphere from Aircraft and Satellites (ARCTAS) campaign of 2008.

b *Origin and Path of the Plume*

During summer 2010, intense drought and high temperatures caused several hundred wildfires in Russia. Indeed, July 2010 was considered the warmest month in Moscow since the beginning of modern meteorological recording 130 years ago. The total vegetated area (forest, vegetation, and peat land) affected by wildfires on Russian territory reached approximately five million hectares by early August 2010, leading to a total CO emission between 34 and 40 Tg CO during July and August 2010 (Yurganov et al., 2011). Images from the Moderate Resolution Imaging Spectroradiometer (MODIS) and the Multiangle Imaging Spectroradiometer (MISR) indicate that smoke extended over approximately 3000 km (from east to west) in early August and sometimes reached altitudes of 12 km, an altitude at which the plume may travel long distances to affect air quality at distant locations.

Figure 2 is a graphical ensemble of evidence illustrating the origin and path of the plume that reached PEARL during August 2010. According to Hybrid Single Particle Lagrangian Integrated Trajectory (HYSPLIT) back-trajectories (Fig. 2a), air masses that arrived on 24 August at PEARL (at 5, 7, and 9 km altitude) (NOAA, 2012) originated in Russia nine days earlier, where the red areas (Fig. 2b) represent the 10-day (9–18 August) average of fire hot spots identified by MODIS (NASA, 2012a). To support this idea, a MODIS image (Fig. 2c) taken on 15 August at 0900 UTC has been superimposed on the area inside the yellow box of Fig. 2b. Comparing Figs 2b and 2c, one can see that all three dots (red, blue, and green, Fig. 2c), representing the air mass

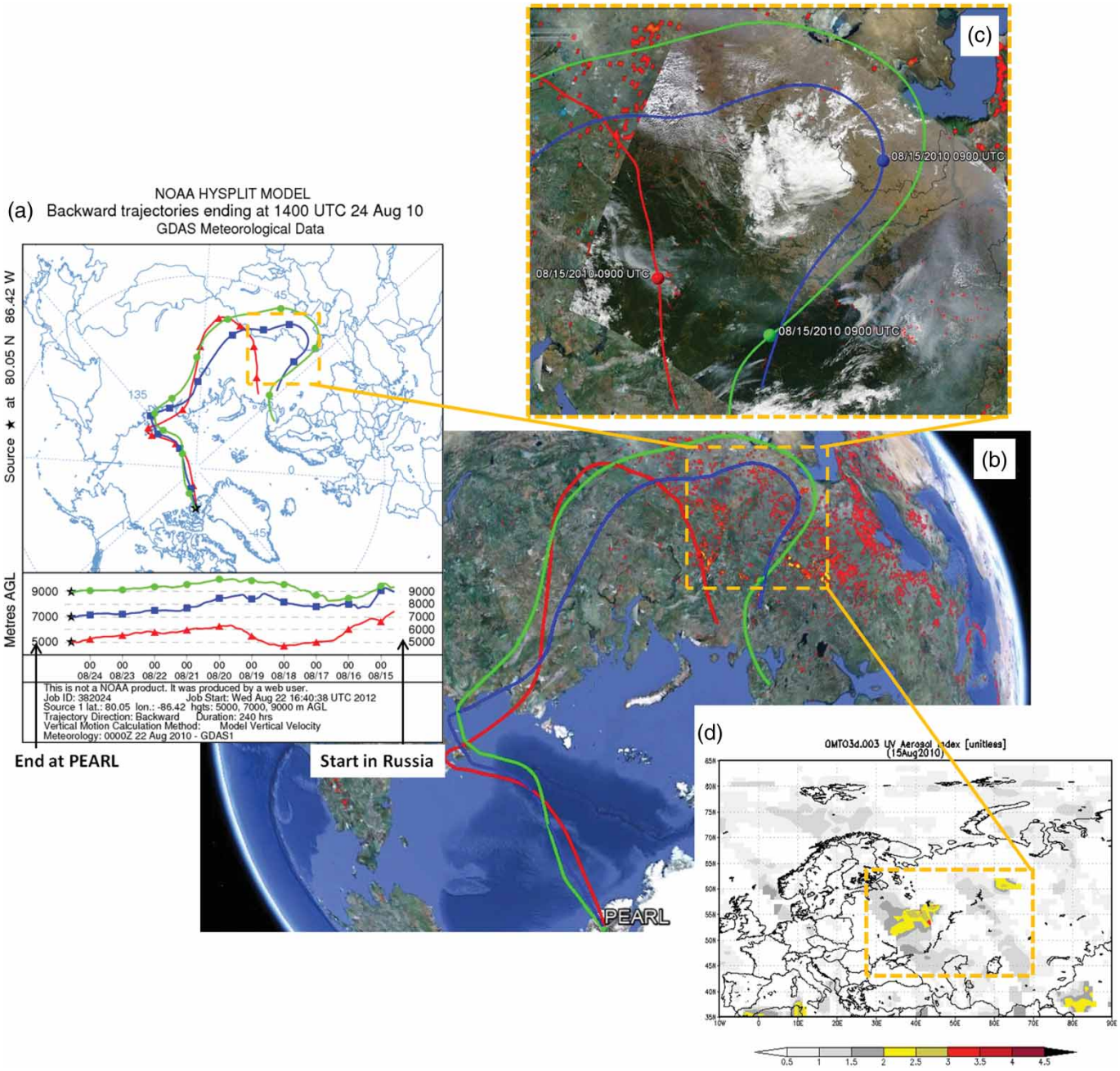

Fig. 2 Images and back-trajectories showing the location of fire events that occurred on 15 August in Russia and arrived at PEARL on 24 August 2010. Evidence of transport of air masses to PEARL: (a) HYSPLIT back-trajectories (courtesy NOAA), and (b) the same trajectories superimposed on a Google Earth map (map provided by Google Earth V 7.0.3.8542, US Dept of State Geographer, Google, 2012, Image Landsat, Data SIO, NOAA, U.S, Navy, NGA, and GEBCO) with MODIS fire hot spots from 9 to 18 August in red. Evidence for Russian fires: (c) MODIS fire image (courtesy NASA), and (d) OMI aerosol index measurements.

locations at the time of the MODIS image, are inside a fire area (red areas) or close to the smoke plume. Additional evidence of intense fire events in the Moscow area is illustrated in Fig. 2d, which presents high values of the ultraviolet aerosol index derived from OMI measurements (NASA, 2012b) in the same fire region (yellow box) and for the same day. Back-trajectories for the beginning of August 2010 confirm that Russian fires affected atmospheric composition at Eureka but are not shown here because their patterns are less clear than the ones for 24 August.

4 Results

a *Trace Gas Correlations*

The HCN total columns from 9 to 30 August 2010 are enhanced by more than 50% compared with the four-year

(2008–11) monthly mean of 5.24×10^{15} molecules cm^{-2} for August measurements at PEARL. Also, all August 2010 measurements (red dots, Figs 3a and 3c) produce a similar slope in the correlation plots; therefore, all these data (from 9 to 30 August) are considered to be fire affected.

The C_2H_6 total columns have been plotted against CO (NDACC-only) for all (1447) spectra recorded in 2010 (Fig. 3a, black) and those for the fire period of August 2010 (Fig. 3a, red). Columns of C_2H_6 and CO are correlated over the year because of their common sink through reaction with OH (Rinsland et al., 1998, 1999, 2000); therefore, the seasonal variability of these molecules is identical throughout the year, with maxima in winter–spring (February–March) and minima in summer–fall (August–September) (Zhao et al., 2002). However, the correlation slope for the August columns differs from the annual one. The high correlation ($R = 0.94$) between C_2H_6 and CO total columns is consistent for all 58 spectra recorded during the fire period (Fig. 3b). Figure 3c shows the HCN total columns measured during all of 2010 (1578 spectra) plotted against the co-located (NDACC-only) measurements of CO. No correlation is seen between HCN and CO total columns throughout the year because different atmospheric chemistry processes control the abundance of these two molecules, but a correlation is present in the August data (red dots, Fig. 3c). Figure 3d confirms this correlation because the coefficient of correlation between the 61 HCN and CO total columns measured in August when the smoke plume from Russia was transported over PEARL is 0.85.

b *Emission Factors for Biomass Burning Species*

The HCN and C_2H_6 emission factors were derived using Eq. (1) and taking the values of the regression slopes as emission ratios. Because CO, HCN, and C_2H_6 lifetimes are relatively long in the atmosphere (around 2, 5, and 1.5 months, respectively, Li et al., 2003; Müller & Brasseur, 1995; Xiao et al., 2008), decay rates of each chemical species were

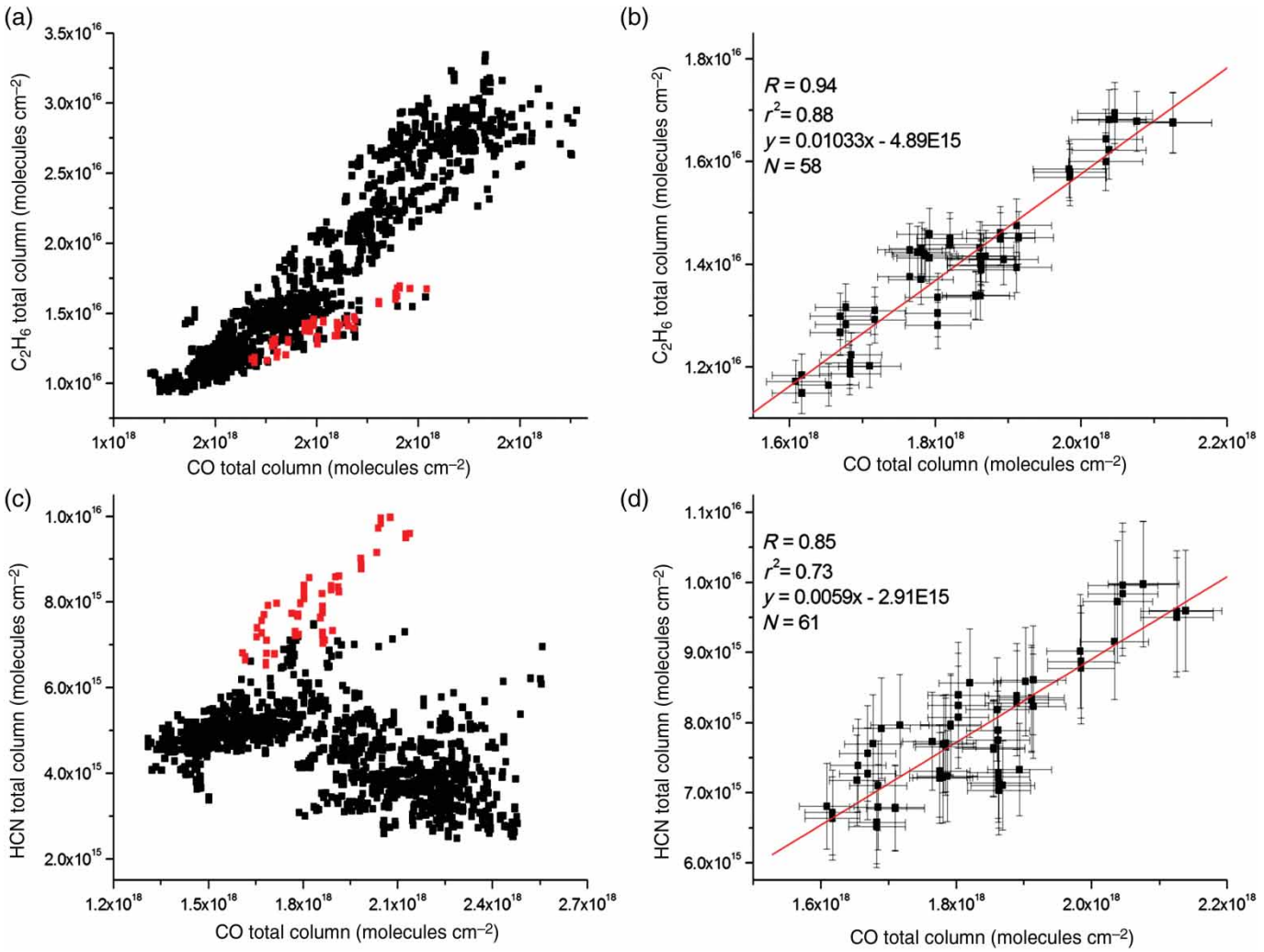

Fig. 3 FTIR total columns of C_2H_6 and HCN plotted against CO total columns. (a) C_2H_6 versus CO for all of 2010 (black) and for August 2010 (red). (b) Correlation plots of C_2H_6 versus CO for August 2010. (c) HCN versus CO for all of 2010 (black) and for August 2010 (red). (d) Correlation plots of HCN versus CO for August 2010. The error bars represent the total uncertainties of the retrievals.

calculated by considering the exponential decrease after nine days, given their relative lifetimes (i.e., for CO the decay rate is exp(−9/61)). Typical lifetimes were used based on values from the literature that assumed climatological OH fields. Therefore, CO, HCN, and C_2H_6 abundances in the nine-day-old aged smoke plume should be 86.3%, 94.2%, and 81.9% of their initial values, respectively, assuming there are no local sources along the trajectories from Russia. Therefore, the measured HCN and C_2H_6 enhancement ratios will differ by a factor of 1.091 (=94.2/86.3) and 0.9488 (=81.9/86.3) relative to the original emission ratios, meaning that those measured ratios are 9.1% higher and 5.1% lower than the emission ratios, respectively. Thus, we have corrected the measured enhancement ratios by taking into account the effect of the aging of the smoke plume in order to derive equivalent emission ratios. Because the uncertainty in the correction is small compared with other uncertainties, our equivalent emission ratios can be compared with other emission ratios found in the literature.

For comparison with previous studies, our corrected enhancement ratios (i.e., equivalent emission ratios) were converted into equivalent emission factors using Eq. (1). In order to compare our results with others, a representative dataset of EF_x was selected, including ground-based (Griffin et al., 2013; Paton-Walsh et al., 2005), satellite (Rinsland et al., 2007; Tereszchuk et al., 2012), and aircraft (Goode et al., 2000; Le Breton et al., 2013; Lewis et al., 2013; Simpson et al., 2011) measurements, as well as compilations from numerous other data sources (Akagi et al., 2011; Andreae & Merlet, 2001) for boreal and extratropical forests. The latter two studies contain a comprehensive set of emission factors from the burning of numerous vegetation types derived from various measurement platforms. The $EF_{C_2H_6}$ and EF_{HCN} from Akagi et al. (2011) were estimated from a combination of ground-based in situ (with a mean value of $EF_{C_2H_6} = 3.0 \pm 2.3$ g kg^{-1} and $EF_{HCN} = 2.5 \pm 1.5$ g kg^{-1}) and airborne measurements (with a mean value of $EF_{C_2H_6} = 0.6 \pm 0.3$ g kg^{-1} and $EF_{HCN} = 0.9 \pm 0.3$ g kg^{-1}). Their reported standard deviations represent variability between studies whereas they are from the 1-sigma uncertainty for the single studies listed in Table 1. Because different values of EF_{CO} were used to calculate EF_x in those studies, ER_x is also reported when available (Table 1).

Our equivalent $ER_{C_2H_6}$ (0.0108 ± 0.0036) is higher than values found in the literature, which is consistent with the fact that fires emits more non-methane hydrocarbons than previously thought (Akagi et al., 2011). However, even if our value is in good agreement with the ground-based and satellite measurements reported by Griffin et al. (2013) and Rinsland et al. (2007), it is higher than emission ratios derived from aircraft measurements reported by Lewis et al. (2013), Simpson et al. (2011), and Goode et al. (2000). This may be caused by potential biases in the measurement techniques and/or the different geometry employed in the sampling that biases the measurements to one stage of burning over another, for example, aircraft measure over a certain altitude range, which might be biased toward flaming combustion often injected into the upper troposphere, whereas a ground-based FTIR measures the total columns from the surface, which might be biased toward smouldering combustion (Hurst et al., 1994). Because this pattern is not seen when comparing our ER_{HCN} with others, the reason for our high value of $ER_{C_2H_6}$ is not yet clear, and these discrepancies may reflect the natural variability of the emissions. Indeed, our equivalent ER_{HCN} (0.0054 ± 0.0022) lies within the range of all other values.

Table 1. Emission factors (g kg^{-1}) and emission ratios for C_2H_6 and HCN calculated in this study alongside those found in the literature.

				ER_x		EF_x	
	Platform	Vegetation Type	EF_{CO}[a]	C_2H_6	HCN	C_2H_6	HCN
This study	Ground-based[b]	Boreal	127 ± 45	0.0108 ± 0.0036	0.0054 ± 0.0022	1.47 ± 0.50	0.66 ± 0.27
		Extratropical	107 ± 37			1.24 ± 0.44	0.56 ± 0.21
Akagi et al. (2011)	Compilation	Boreal	127 ± 45	—	—	1.79 ± 1.14	1.52 ± 0.81
Andreae and Merlet (2001)	Compilation	Extratropical	107 ± 37	—	—	0.73 ± 0.41[c]	0.81[c]
Le Breton et al. (2013)	Aircraft[d]	Boreal	—	—	0.0038 ± 0.0002	—	—
Lewis et al. (2013)	Aircraft[d]	Boreal	—	0.0051 ± 0.0035	—	—	—
Simpson et al. (2011)	Aircraft[e]	Boreal	113 ± 72	0.0046 ± 0.0090	0.0082 ± 0.0020	0.56 ± 0.13	0.89 ± 0.29
Goode et al. (2000)	Aircraft[f]	Boreal	88.8	0.0073	0.0069	0.66	0.61
Rinsland et al. (2007)	Satellite[g]	Boreal	86 ± 17	0.0098 ± 0.0008	0.0024 ± 0.0003	0.91 ± 0.19	0.20 ± 0.05
Tereszchuk et al. (2012)	Satellite[d]	Boreal	—	0.0069 ± 0.0023	0.0027 ± 0.0018	—	—
Griffin et al. (2013)	Ground-based[d]	Boreal	122 ± 45	0.0100 ± 0.0060	—	1.35 ± 0.51	—
Paton-Walsh et al. (2005)	Ground-based[h]	Temperate	107 ± 37	0.0023 ± 0.0005	0.0042 ± 0.0016	0.26 ± 0.11	0.43 ± 0.22

[a]Used to convert ER_x to EF_x (g kg^{-1}).
[b]Fire from Russia, measurements made in the Arctic region (PEARL, 80.05°N, Eureka).
[c]Updates from M. O. Andreae (see Paton-Walsh et al., 2005).
[d]Fire from Canada, measurements made over northwestern Ontario, Canada (BOReal forest fires on Tropospheric oxidants over the Atlantic using Aircraft and Satellites (BORTAS) campaign).
[e]Fire from Canada, measurements made over Canada (ARCTAS campaign).
[f]Fire from Alaska, measurements over Alaska.
[g]Fire from Alaska and western Canada, measurements over Alaska and Canada (between 50.2°N and 67.8°N).
[h]Fire from Australian temperate forest, measurements at Wollongong, Australia (35.5°S).

The emission factors of C_2H_6 calculated in this study are 1.47 ± 0.50 g kg^{-1} when considering the EF_{CO} value from Akagi et al. (2011) and 1.24 ± 0.44 g kg^{-1} when considering the EF_{CO} value from Andreae and Merlet (2001). Those values are in excellent agreement with the value reported by Griffin et al. (2013) and agree well with satellite measurements in Rinsland et al. (2007), as well as with the mean for boreal forest fires found in Akagi et al. (2011) (see Table 1). However, our values of $EF_{C_2H_6}$ are at least five times higher than the $EF_{C_2H_6}$ values for Australian temperate forest calculated from ground-based FTIR measurements because the fuel in Australia is different, and the Australian vegetation (predominantly Eucalyptus trees) has low biomass burning emissions of C_2H_6 (Paton-Walsh et al., 2005).

For HCN, emission factors of 0.66 ± 0.27 g kg^{-1} and 0.56 ± 0.21 g kg^{-1} (using the EF_{CO} value from Akagi et al. (2011) and Andreae and Merlet (2001), respectively) were calculated in this study (Table 1), which agree within combined errors with all previous studies referenced here, except that of Rinsland et al. (2007). Rinsland et al. (2007) calculated an EF_{HCN} approximately five times lower than the value of 0.92 g kg^{-1} derived from laboratory measurements of boreal fuels and reported by Bertschi et al. (2003), which is not in agreement with the mean for boreal forest fires found in Akagi et al. (2011). This low value may be partially attributed to the relatively low EFco of 86 ± 17 g kg^{-1} (derived from the mean of airborne measurements from an Alaskan wildfire reported in Nance, Hobbs, Radke, and Ward (1993) and Goode et al. (2000)) used in the Rinsland et al. (2007) study to estimate EF_{HCN}. In addition, a recent study provided ER_{HCN} for very different but globally important fuel types (Akagi et al., 2013, their Fig. 10) and highlighted the fact that ER_{HCN} has a high fuel dependence, ranging from below detection level for pure wood in cooking fires (Christian et al., 2010) to 3% or greater for some peat samples (Akagi et al., 2011). However, the mean ER_{HCN} reported by Akagi et al. (2013) ranges from 0.0063 to 0.0095 which agrees well, within the uncertainties, with our ER_{HCN}.

5 Conclusions

In this study we used ground-based FTIR measurements of biomass burning products (CO, HCN, and C_2H_6) taken in the high Arctic to assess emission ratios relative to CO for the boreal forest. With several independent sources of information (AODs, HYSPLIT back-trajectories, MODIS images, OMI aerosol index, and IASI CO total columns), we confirmed that the FTIR measurements recorded in August 2010 were inside a persistent smoke plume transported from Russia. The equivalent emission factor of C_2H_6 (1.47 ± 0.50 g kg^{-1}) found in our study is in agreement with the mean values reported in the compilation studies of Akagi et al. (2011) and Andreae and Merlet (2001), the satellite measurements of Rinsland et al. (2007), and the ground-based measurements of Griffin et al. (2013) for the boreal forest. However, our C_2H_6 emission factor is found to be higher than values derived from airborne observations (Goode et al., 2000; Simpson et al., 2011), possibly because of the different sampling method. Our C_2H_6 emission factor is also larger than the value derived from ground-based observations (Paton-Walsh et al., 2005) possibly because of the different type of fuel burned in Australia. Our equivalent emission factor of HCN (0.66 ± 0.27 g kg^{-1}) is in agreement with all studies referenced here (Akagi et al., 2011; Andreae & Merlet, 2001; Paton-Walsh et al., 2005; Simpson et al., 2011), with the exception of Rinsland et al. (2007), who reported a lower value that might be consistent with the real variability of HCN emissions (Akagi et al., 2013). Given the large range of values found in the literature, this study adds new observations to the sparse dataset of emission factors that have been reported and compiled in the literature. Future work will focus on the detection of other fire events as well as retrieval of other trace gases from smoke spectra recorded at Eureka.

Acknowledgements

The PEARL Bruker 125HR and sunphotometer measurements at Eureka were made by the Canadian Network for the Detection of Atmospheric Change (CANDAC), which was supported by the Atlantic Innovation Fund/Nova Scotia Research and Innovation Trust (AIF/NSRIT), the Canadian Foundation for Innovation (CFI), the Canadian Foundation for Climate and Atmospheric Sciences (CFCAS), the Canadian Space Agency (CSA), Environment Canada (EC; including operational support by Ihab Abboud of AEROCAN), Government of Canada International Polar Year (IPY) funding, the Natural Sciences and Engineering Research Council (NSERC), the Ontario Innovation Trust (OIT), the Ontario Research Fund (ORF), the Polar Continental Shelf Program (PCSP), and the Fonds de recherché, Nature et technologie (FQRNT). The authors wish to thank the staff at the Eureka weather station and CANDAC for the logistical and on-site support provided. Thanks to Rodica Lindenmaier, Rebecca Batchelor, PEARL Site Manager Pierre Fogal, and CANDAC/PEARL operators Ashley Harrett, Alexei Khmel, Paul Loewen, Keith MacQuarrie, Oleg Mikhailov, and Matt Okraszewski, for their invaluable assistance in maintaining the Bruker 125HR and for taking measurements. Matthieu Pommier and the French atmospheric database Ether are acknowledged for providing the Infrared Atmospheric Sounding Interferometer (IASI) data. The authors also acknowledge the National Oceanic and Atmospheric Administration-Air Resources Laboratory (NOAA-ARL) for access to the Hybrid Single Particle Lagrangian Integrated Trajectory (HYSPLIT) model, and the National Aeronautics and Space Administration (NASA) for its Moderate Resolution Imaging Spectrometer (MODIS) and Ozone Monitoring Instrument (OMI) imagery products available from their Rapidfire website and from the Giovanni online data system, developed and maintained by the NASA Goddard Earth Sciences (GES)

Data and Information Services Center (DISC). The visit of C. Paton-Walsh to the University of Toronto to collaborate on this study was funded by the Australian Research Council (ARC) as part of project DP110101948.

References

Akagi, S. K., Yokelson, R. J., Burling, I. R., Meinardi, S., Simpson, I., Blake, D. R., … Weise, D. R. (2013). Measurements of reactive trace gases and variable O_3 formation rates in some South Carolina biomass burning plumes. *Atmospheric Chemistry and Physics*, *13*, 1141–1165. doi:10.5194/acp-13-1141-2013

Akagi, S. K., Yokelson, R. J., Wiedinmyer, C., Alvarado, M. J., Reid, J. S., Karl, T., … Wennberg, P. O. (2011). Emission factors for open and domestic biomass burning for use in atmospheric models. *Atmospheric Chemistry and Physics*, *11*, 4039–4072. doi:10.5194/acp-11-4039-2011

Amiro, B. D., Todd, J. B., Wotton, B. M., Logan, K. A., Flannigan, M. D., Stocks, B. J., … Hirsh, K. G. (2001). Direct carbon emissions from Canadian forest fires, 1959–1999. *Canadian Journal of Forest Research*, *31*, 512–525. doi:10.1139/x2012-104

Andreae, M. O., & Merlet, P. (2001). Emission of trace gases and aerosols from biomass burning. *Global Biogeochemical Cycles*, *15*, 955–966. doi:10.1029/2000GB001382

Batchelor, R. L., Strong, K., Lindenmaier, R. L., Mittermeier, R., Fast, H., Drummond, J. R., & Fogal, P. F. (2009). A new Bruker IFS 125HR FTIR spectrometer for the Polar Environment Atmospheric Research Laboratory at Nunavut, Canada: Measurements and comparison with the existing Bomem DA8 spectrometer. *Journal of Atmospheric and Oceanic Technology*, *26*, 1328–1340. doi:10.1175/2009JTECHA1215.1

Bertschi, I., Yokelson, R. J., Ward, D. E., Babbitt, R. E., Susott, R. A., Goode, J. G., & Hao, W. M. (2003). Trace gas and particle emissions from fires in large diameter and belowground biomass fuels. *Journal of Geophysical Research*, *108*(D13), 8472. doi:10.1029/2002JD002100

Christian, T. J., Yokelson, R. J., Cardenas, B., Molina, L. T., Engling, G., & Hsu, S.-C. (2010). Trace gas and particle emissions from domestic and industrial biofuel use and garbage burning in central Mexico. *Atmospheric Chemistry and Physics*, *10*, 565–584. doi:10.5194/acp10-565-2010

Colarco, P. R., Schoeberl, M. R., Doddridge, B. G., Marufu, L. T., Torres, O., & Welton, E. J. (2004). Transport of smoke from Canadian forest fires to the surface near Washington, D.C.: Injection height, entrainment, and optical properties. *Journal of Geophysical Research*, *109*(D6), D06203. doi:10.1029/2003JD004248

Eremenko, M., Dufour, G., Foret, G., Keim, C., Orphal, J., Beekmann, M., … Flaud, J.-M. (2008). Tropospheric ozone distributions over Europe during the heat wave in July 2007 observed from infrared nadir spectra recorded by IASI. *Geophysical Research Letters*, *35*, L18805. doi:10.1029/2008GL034803

Eyring, V., Waugh, D. W., Bodeker, G. E., Cordero, E., Akiyoshi, H., Austin, J., … Yoshiki, M. (2007). Multimodel projections of stratospheric ozone in the 21st century. *Journal of Geophysical Research*, *112*, D16303. doi:10.1029/2006JD008332

Goode, J. G., Yokelson, R. J., Ward, D. E., Susott, R. A., Babbitt, R. E., Davies, M. A., & Hao, W. M. (2000). Measurements of excess O_3, CO_2, CO, CH_4, C_2H_4, C_2H_2, HCN, NO, NH_3, HCOOH, CH_3COOH, HCHO, and CH_3OH in 1997 Alaskan biomass burning plumes by airborne Fourier transform infrared spectroscopy (AFTIR). *Journal of Geophysical Research*, *105*(D17), 22147–22166. doi:10.1029/2000JD900287

Griffin, D., Walker, K. A., Franklin, J. E., Parrington, M., Whaley, C., Hopper, J., … Weaver, D. (2013). Investigation of CO, C_2H_6 and aerosols in a boreal fire plume over eastern Canada during BORTAS 2011 using ground- and satellite-based observations, and model simulations. *Atmospheric Chemistry and Physics Discussions*, *13*, 11071–11109. doi:10.5194/acpd-13-11071-2013

Holben, B. N., Holben, B. N., Eck, T. F., Slutsker, I., Tanre, D., Buis, J. P., … Smirnov, A. (1998). AERONET – A federated instrument network and data archive for aerosol characterization. *Remote Sensing of Environment*, *66*, 1–16.

Hurst, D. F., Griffith, D. W. T., & Cook, G. D. (1994). Trace gas emissions from biomass burning in tropical Australian savannas. *Journal of Geophysical Research*, *99*(D8), 16441–16456. doi:10.1029/94JD00670

Hurtmans, D., Coheur, P.-F., Wespes, C., Clarisse, L., Scharf, O., Clerbaux, C., … Turquety, S. (2012). FORLI radiative transfer and retrieval code for IASI. *Journal of Quantitative Spectroscopy and Radiative Transfer*, *113*, 1391–1408. doi:10.1016/j.jqsrt.2012.02.036

IPCC (Intergovernmental Panel on Climate Change). (2007). Coupling between changes in the climate system and biogeochemistry (Ch. 7). In S. Solomon, D. Quin, M. Manning, Z. Chen, M. Marquis, K. B. Averyt, M. Tignor, & H. L. Miller (Eds.), *Climate Change 2007: The physical science basis* (pp. 500–567). Cambridge, UK: Cambridge University Press.

Kerzenmacher, T., Dils, B., Kumps, N., Blumenstock, T., Clerbaux, C., Coheur, P.-F., … De Mazière, M. (2012). Validation of IASI FORLI carbon monoxide retrievals using FTIR data from NDACC. *Atmospheric Measurement Techniques Discussions*, *5*, 3973–4002. doi:10.5194/amtd-5-3973-2012

Le Breton, M., Bacak, A., Muller, J. B. A., O'Shea, S. J., Xiao, P., Ashfold, M. N. R., … Percival, C. J. (2013). Airborne HCN measurements from biomass burning. *Atmospheric Chemistry and Physics Discussions*, *13*, 5649–5685. doi:10.5194/acpd-13-5649-2013

Lewis, A. C., Evans, M. J., Hopkins, J. R., Punjabi, S., Read, K. A., Purvis, R. M., … Parrington, M. (2013). The influence of biomass burning on the global distribution of selected non-methane organic compounds. *Atmospheric Chemistry and Physics*, *13*, 851–867. doi:10.5194/acp-13-851-2013

Li, Q., Jacob, D. J., Yantosca, R. M., Heald, C. L., Singh, H. B., Koike, M., … Streets, D. G. (2003). A global three-dimensional model analysis of the atmospheric budgets of HCN and CH_3CN: Constraints from aircraft and ground measurements. *Journal of Geophysical Research*, *108*(D21), 8827. doi:10.1029/2002JD003075

Lindenmaier, R. (2012). *Studies of Arctic middle atmosphere chemistry using infrared absorption spectroscopy* (PhD thesis). University of Toronto, Toronto, Canada.

Müller, J.-F., & Brasseur, G. (1995). IMAGES: A three-dimensional chemical transport model of the global troposphere. *Journal of Geophysical Research*, *100*(D8), 16445–16490. doi:10.1029/94JD03254

Nance, J. D., Hobbs, P. V., Radke, L. F., & Ward, D. E. (1993). Airborne measurements of gases and particles from an Alaskan wildfire. *Journal of Geophysical Research*, *98*, 14873–14882. doi: 10.1029/93JD01196

NASA (National Aeronautics and Space Administration). (2012a). *Global fire maps*. Goddard Space Flight Center, LANCE-MODIS. Retrieved from http://lance-modis.eosdis.nasa.gov/cgi-bin/imagery/firemaps.cgi

NASA (National Aeronautics and Space Administration). (2012b). *OMI/Aura Online Visualization and Analysis: Daily Level 3 Global Gridded Products*. Retrieved from http://gdata1.sci.gsfc.nasa.gov/daac-bin/G3/gui.cgi?instance_id=omi

NOAA (National Oceanic and Atmospheric Administration). (2012). *HYSPLIT - Hybrid Single Particle Lagrangian Integrated Trajectory Model*. Air Resources Laboratory. Retrieved from http://ready.arl.noaa.gov/HYSPLIT.php

O'Neill, N. T., Eck, T. F., Smirnov, A., Holben, B. N., & Thulasiraman, S. (2003). Spectral discrimination of coarse and fine mode optical depth. *Journal of Geophysical Research*, *108*(D17), 4559–4573. doi:10.1029/2002JD002975

O'Neill, N. T., Pancrati, O., Baibakov, K., Eloranta, E., Batchelor, R. L., Freemantle, J., … Lindenmaier, R. (2008). Occurrence of weak, submicron, tropospheric aerosol events at high Arctic latitudes. *Geophysical Research Letters*, *35*, L14814. doi:10.1029/2008GL033733

Paton-Walsh, C., Deutscher, N. M., Griffith, D. W. T., Forgan, B. W., Wilson, S. R., Jones, N. B., & Edwards, D. P. (2010). Trace gas emissions from

savanna fires in Northern Australia. *Journal of Geophysical Research*, *115*, D16314. doi:10.1029/2009JD013309

Paton-Walsh, C., Jones, N. B., Wilson, S. R., Harverd, V., Meier, A., Griffith, D. W. T., & Rinsland, C. P. (2005). Measurements of trace gas emissions from Australian forest fires and correlations with coincident measurements of aerosol optical depth. *Journal of Geophysical Research*, *110*, D24305. doi:10.1029/2005JD006202

Paton-Walsh, C., Jones, N. B., Wilson, S. R., Meier, A., Deutscher, N., & Griffith, D. (2004). Trace gas emissions from biomass burning inferred from aerosol optical depth. *Geophysical Research Letters*, *31*(5), L05116. doi:10.1029/2003GL018973

Preston, C. M., & Schmidt, M. W. I. (2006). Black (pyrogenic) carbon: A synthesis of current knowledge and uncertainties with special consideration of boreal regions. *Biogeosciences*, *3*, 397–420. doi:10.5194/bg-3-397-2006

Rinsland, C. P., Dufour, G., Boone, C. D., Bernath, P. F., Chiou, L., Coheur, P. F., … Clerbaux, C. (2007). Satellite boreal measurements over Alaska and Canada during June–July 2004: Simultaneous measurements of upper tropospheric CO, C_2H_6, HCN, CH_3Cl, CH_4, C_2H_2, CH_3OH, HCOOH, OCS, and SF_6 mixing ratios. *Global Biogeochemical Cycles*, *21*, GB3008. doi:10.1029/2006GB002795

Rinsland, C. P., Goldman, A., Murcray, F. J., Stephen, T. M., Pougatchev, N. S., Fishman, J., … Connor, B. J. (1999). Infrared solar spectroscopic measurements of free tropospheric CO, C_2H_6, and HCN above Mauna Loa, Hawaii: Seasonal variations and evidence for enhanced emissions from the southeast Asian tropical fires of 1997–1998. *Journal of Geophysical Research*, *104*(D15), 18667–18680. doi:10.1029/1999JD900366

Rinsland, C. P., Jones, N. B., Connor, B. J., Logan, J. A., Pougatchev, N. S., Goldman, A., … Demoulin, P. (1998). Northern and southern hemisphere ground-based infrared spectroscopic measurements of tropospheric carbon monoxide and ethane. *Journal of Geophysical Research*, *103*(D21), 28, 197–28, 217. doi:10.1029/98JD02515

Rinsland, C. P., Mahieu, E., Zander, R., Demoulin, P., Forrer, J., & Buchmann, B. (2000). Free tropospheric CO, C_2H_6, and HCN above central Europe: Recent measurements from the Jungfraujoch station including the detection of elevated columns during 1998. *Journal of Geophysical Research*, *105*, 24,235–24,249. doi:10.1029/2000JD900371

Rodgers, C. D. (2000). *Inverse methods for atmospheric sounding: Theory and practice, series on atmospheric, oceanic and planetary physics* (Vol. 2). Singapore: World Scientific Publishing Co.

Rothman, L. S., Gordon, I. E., Barbe, A., Chris Benner, D., Bernath, P. F., Birk, M., … Vander Auwera, J. (2009). The HITRAN 2008 molecular spectroscopic database. *Journal of Quantitative Spectroscopy and Radiative Transfer*, *110*, 533–572. doi:10.1016/j.jqsrt.2009.02.013

Saha, A., O'Neill, N. T., Eloranta, E., Stone, R. S., Eck, T. F., Zidane, S., … McArthur, L. J. B. (2010). Pan-Arctic sunphotometry during the ARCTAS-A campaign of April 2008. *Geophysical Research Letters*, *37*, L05803. doi:10.1029/2009GL041375

Shindell, D. T., Shindell, D. T., Chin, M., Dentener, F., Doherty, R. M., Faluvegi, G., … Zuber, A. (2008). A multi-model assessment of pollution transport to the Arctic. *Atmospheric Chemistry and Physics*, *8*, 5353–5372. doi:10.5194/acp-8-5353-2008

Simpson, I. J., Akagi, S. K., Barletta, B., Blake, N. J., Choi, Y., Diskin, G. S., … Blake, D. R. (2011). Boreal forest fire emissions in fresh Canadian smoke plumes: C_1–C_{10} volatile organic compounds (VOCs), CO_2, CO, NO_2, NO, HCN and CH_3CN. *Atmospheric Chemistry and Physics*, *11*, 6445–6463. doi:10.5194/acp-11-6445-2011

Soja, A. J., Tchebakova, N. M., French, N. H. F., Flannigan, M. D., Shugart, H. H., Stocks, B. J., … Stackhouse, P. W., Jr. (2007). Climate-induced boreal forest change: Predictions versus current observations. *Global and Planetary Change*, *56*(3–4), 274–296. doi:10.1016/j.gloplacha.2006.07.028

Tereszchuk, K. A., Gonzalez Abad, G., Clerbaux, C., Hadji-Lazaro, J., Hurtmans, D., Coheur, P.-F., & Bernath, P. F. (2012). ACE-FTS observations of pyrogenic trace species in boreal biomass burning plumes during BORTAS. *Atmospheric Chemistry and Physics Discussions*, *12*, 31629–31661. doi:10.5194/acpd-12-31629-2012

Turquety, S., Hurtmans, D., Hadji-Lazaro, J., Coheur, P.-F., Clerbaux, C., Josset, D., & Tsamalis, C. (2009). Tracking the emission and transport of pollution from wildfires using the IASI CO retrievals: Analysis of the summer 2007 Greek fires. *Atmospheric Chemistry and Physics*, *9*, 4897–4913. doi:10.5194/acp-9-4897-2009

Vigouroux, C., Stavrakou, T., Whaley, C., Dils, B., Duflot, V., Hermans, C., … De Mazière, M. (2012). FTIR time-series of biomass burning products (HCN, C_2H_6, C_2H_2, CH_3OH, and HCOOH) at Reunion Island (21°S, 55°E) and comparisons with model data. *Atmospheric Chemistry and Physics Discussions*, *12*, 13733–13786. doi:10.5194/acpd-12-13733-2012

Wunch, D., Toon, G. C., Blavier, J.-F.L., Washenfelder, R., Notholt, J., Connor, B. J., … Wennberg, P. O. (2011). The Total Carbon Column Observing Network. *Philosophical Transactions of the Royal Society A*, *369*, 2087–2112. doi:10.1098/rsta.2010.0240

Xiao, Y., Logan, J. A., Jacob, D. J., Hudman, R. C., Yantosca, R., & Blake, D. R. (2008). Global budget of ethane and regional constraints on US sources. *Journal of Geophysical Research*, *113*, D21306. doi:10.1029/2007JD009415

Yurganov, L. N., Rakitin, V., Dzhola, A., August, T., Fokeeva, E., George, M., … Strow, L. (2011). Satellite- and ground-based CO total column observations over 2010 Russian fires: Accuracy of top-down estimates based on thermal IR satellite data. *Atmospheric Chemistry and Physics*, *11*, 7925–7942. doi:10.5194/acp-11-7925-2011

Zhao, Y., Strong, K., Kondo, Y., Koike, M., Matsumi, Y., Irie, H., … Murata, I. (2002). Spectroscopic measurements of tropospheric CO, C_2H_6, C_2H_2, and HCN in northern Japan. *Journal of Geophysical Research*, *107*(D18), 4343. doi:10.1029/2001JD000748